J|A|C|S
ARTICLES

Published on Web 10/01/2009

FePt Nanoparticles as an Fe Reservoir for Controlled Fe Release and Tumor Inhibition

Chenjie Xu,[†] Zhenglong Yuan,[‡] Nathan Kohler,[†] Jaemin Kim,[†] Maureen A. Chung,[‡] and Shouheng Sun*,[†]

Department of Chemistry, Brown University, Providence, Rhode Island 02912, Department of Surgery, Rhode Island Hospital, Brown University, Providence, Rhode Island 02903

Received July 16, 2009; E-mail: ssun@brown.edu

Abstract: Chemically disordered face centered cubic (fcc) FePt nanoparticles (NPs) show the controlled release of Fe in low pH solution. The released Fe catalyzes H_2O_2 decomposition into reactive oxygen species within cells, causing fast oxidation and deterioration of cellular membranes. Functionalized with luteinizing hormone-releasing hormone (LHRH) peptide via phospholipid, the fcc-FePt NPs can bind preferentially to the human ovarian cancer cell line (A2780) that overexpresses LHRH receptors and exhibit high toxicity to these tumor cells. In contrast, the fcc-FePt NPs pre-etched in the low pH (4.8) buffer solution show nonappreciable cytotoxicity. The work demonstrates that fcc-FePt NPs may function as a new type of agent for controlled cancer therapy.

Introduction

Magnetic nanoparticles (NPs) have demonstrated strong promise toward the development of new targeted agents for cancer diagnosis and therapy.[1] Immobilized with chemotherapeutic molecules and targeting agents, these magnetic NPs allow real-time monitoring of drug treatment. However, multiple step conjugation of therapeutic and targeting agents to a NP is often a low yield process, and the presence of both drug and targeting molecules on the same NP surface may interfere with the targeting capability and the subsequent uptake of the NP−drug conjugates. Recent development in NP research allows the synthesis of various composite NPs with core/shell, alloy, and dumbbell-like structures[2] that offer a promising solution to this problem encountered in the single component magnetic NPs. For example, dumbbell-like Au−Fe_3O_4 NPs were applied to couple the anticancer drug platin on Au and Herceptin antibody on Fe_3O_4 with the number of platin molecules and antibody being controlled by the size of Au and Fe_3O_4 NPs.[3] The composite NPs demonstrated the targeted specific delivery of platin to breast tumor cells (SK-BR-3). Alternatively, core/shell structured FePt/CoS NPs were found to be highly cytotoxic.[4] If utilized as a therapeutic agent, these core/shell NPs might offer an even more promising solution to the multistep conjugation problem in the NP delivery system as one would only need to anchor a targeting agent on the NP surface and the number of targeting molecules could be readily controlled by NP sizes.

Here, we report that face centered cubic (fcc) FePt NPs[5] are subject to low pH etching, releasing Fe that is cytotoxic. The cytotoxicity can be controlled in the targeted tumor cells, and the FePt NPs after Fe release show nonappreciable toxicity. Monodisperse FePt NPs have been studied extensively for potential applications in data storage,[5,6] exchange-spring nanocomposite magnets,[7] biodetection,[8] and fuel cell catalysts.[9] As-synthesized, the FePt NPs adopt a chemically disordered fcc structure that can be converted to a face centered tetragonal (fct) structure via high temperature annealing.[5] In the fcc-FePt, both Fe and Pt atoms are randomly positioned in the structure while in the fct-FePt Fe and Pt atoms form alternating layers stacked along the [001] direction.[10] Such structural difference in fcc-FePt and fct-FePt NPs leads to distinctive property change not only in magnetism[5] but also in chemical stability. In the recent acid resistance test, we found that Fe in the fcc-FePt NPs could be etched away in a dilute HCl solution while fct-FePt NPs were stable against this etching in the same solution.[11] We further noticed that this Fe-release behavior was common for

[†] Department of Chemistry, Brown University.
[‡] Department of Surgery, Rhode Island Hospital.

(1) (a) Lee, J. H.; Huh, Y. M.; Jun, Y.; Seo, J.; Jang, J.; Song, H. T.; Kim, S.; Cho, E. J.; Yoon, H. G.; Suh, J. S.; Cheon, J. *Nat. Med.* **2007**, *13*, 95–99. (b) Jun, Y. W.; Lee, J. H.; Cheon, J. *Angew. Chem., Int. Ed.* **2008**, *47*, 5122–5135. (c) Sun, C.; Lee, J. S. H.; Zhang, M. Q. *Adv. Drug Delivery Rev.* **2008**, *60*, 1252–1265. (d) Mornet, S.; Vasseur, S.; Grasset, F.; Duguet, E. *J. Mater. Chem.* **2004**, *14*, 2161–2175. (e) Pankhurst, Q. A.; Connolly, J.; Jones, S. K.; Dobson, J. *J. Phys. D: Appl. Phys.* **2003**, *36*, R167–R181.
(2) Xu, C. J.; Sun, S. H. *Dalton Trans.* **2009**, 5583–5591.
(3) Xu, C. J.; Wang, B. D.; Sun, S. H. *J. Am. Chem. Soc.* **2009**, *131*, 4216–4217.
(4) Gao, J. H.; Liang, G. L.; Zhang, B.; Kuang, Y.; Zhang, X. X.; Xu, B. *J. Am. Chem. Soc.* **2007**, *129*, 1428–1433.
(5) Sun, S. H.; Murray, C. B.; Weller, D.; Folks, L.; Moser, A. *Science* **2000**, *287*, 1989–1992.
(6) (a) Weller, D.; Doerner, M. F. *Ann. Rev. Mater. Sci.* **2000**, *30*, 611–644. (b) Moser, A.; Takano, K.; Margulies, D. T.; Albrecht, M.; Sonobe, Y.; Ikeda, Y.; Sun, S. H.; Fullerton, E. E. *J. Phys. D: Appl. Phys.* **2002**, R157–R167.
(7) Zeng, H.; Li, J.; Liu, J. P.; Wang, Z. L.; Sun, S. H. *Nature* **2002**, *420*, 395–398.
(8) Gu, H. W.; Ho, P. L.; Tsang, K. W. T.; Wang, L.; Xu, B. *J. Am. Chem. Soc.* **2003**, *125*, 15702–15703.
(9) (a) Chen, W.; Kim, J.; Sun, S. H.; Chen, S. W. *Phys. Chem. Chem. Phys.* **2006**, *8*, 2779–2786. (b) Chen, W.; Kim, J.; Sun, S. H.; Chen, S. W. *Langmuir* **2007**, *23*, 11303–11310. (c) Chen, W.; Kim, J.; Sun, S. H.; Chen, S. W. *J. Phys. Chem. C* **2008**, *112*, 3891–3898.
(10) Sun, S. H. *Adv. Mater.* **2006**, *18*, 393–403.
(11) Kim, J. M.; Rong, C. B.; Liu, J. P.; Sun, S. H. *Adv. Mater.* **2009**, *21*, 906–909.

 10.1021/ja905938a CCC: $40.75

the fcc-FePt NPs even in low pH solutions and the released Fe could catalyze H_2O_2 decomposition into reactive oxygen species (ROS) that are highly reactive for lipid membrane oxidation. Such Fe-catalyzed ROS formation and its toxicity to cellular systems have long been known, and an uncontrolled accumulation of Fe in cellular environments can lead to serious cellular damage and cell death.[12] Through FePt NPs, we are able to control intracellular accumulation of Fe and cytotoxicity in human cancer cell lines. We demonstrate that fcc-FePt NPs are capable of releasing Fe in low pH (4.8) environments, while remaining chemically inert in neutral pH (7.4) conditions. The released Fe within a cell catalyzes H_2O_2 decomposition into ROS, leading to fast membrane lipid oxidation and cell death. Coupled with luteinizing hormone-releasing hormone (LHRH) peptide,[13] the fcc-FePt NPs bind preferentially to the human ovarian cancer cells (A2780) and exhibit the target-enhanced cytotoxicity to these tumor cells. The work proves that fcc-FePt NPs can serve as a new type of therapeutic agent from which Fe is stored in neutral pH conditions but is released in low pH intracellular environments. Such fcc-FePt NPs can in principle be functionalized with any kind of cancer-targeting antibody or peptide and are therefore promising for future target-specific therapeutic applications.

Experimental Section

General. LHRH peptides (Gln-His-Trp-Ser-Tyr-DLys(DCys)-Leu-Arg-Pro-NHEt, MW = 1344.5) were synthesized according to Minko's design[13] by American Peptide (Sunnyvale, CA). Methyl-PEG_4-amine, 1-ethyl-3-[3-dimethylaminopropyl]carbodiimide hydrochloride (EDC) and *N*-hydroxysulfosuccinimide (sulfo-NHS) were purchased from Thermo Scientific. 2′,7′-Dichlorodihydrofluorescein diacetate (DCFH-DA) and C11-BODIPY were purchased from Molecular Probes. All biological buffers were purchased from Fisher Scientific. Deionized (DI) water was purified by a Millipore Milli-DI water purification system. All other chemicals were purchased from Sigma-Aldrich and used without further purification. Transmission electron microscopy (TEM) images were acquired on a Philips EM 420 (120 kV). Fluorescent images were obtained on a Leica TCS SP2 AOBS spectral confocal microscope. Hydrodynamic sizes of NPs were measured by Malvern Zeta Sizer S90 dynamic light scattering instrument. Fe and Pt concentrations in the solutions were determined by inductively coupled plasma atomic emission spectroscopy (ICP-AES) (Jobin-Yvon JY2000).

Cell Culture. All human cancer cell lines were obtained from ATCC and cultured at 37 °C in 5% CO_2 in 75 cm^2 flasks (Corning) containing Dulbecco's Modified Eagle Medium (DMEM), 1% antibiotics, and 10% fetal bovine serum (FBS). Cells were used at 5−15 passages.

FePt NP Synthesis. $Pt(acac)_2$ (180 mg, 0.48 mmol) in 10 mL of benzyl ether was heated to 110 °C under an Ar atmosphere. Oleylamine (1.4 mL, 4 mmol) and oleic acid (1.4 mL, 4 mmol) were added. After 5 min, the Ar flow was stopped, and the reaction system was protected under an Ar blanket. $Fe(CO)_5$ (0.13 mL, 1 mmol) was added to the solution that was then heated to 225 °C at a heating rate of 5 °C/min and kept at 225 °C for 1 h. A gentle Ar flow was allowed into the reaction system to remove the low boiling point byproduct. Under an Ar blanket, the solution was heated to 300 °C and refluxed for 1 h before it was cooled to room temperature. The fcc-FePt NPs were separated and purified as described.[14]

Fe_3O_4 NP Synthesis. $Fe(acac)_3$ (706 mg, 2 mmol) was dissolved in a mixture of 10 mL of benzyl ether and 10 mL of oleylamine. The solution was dehydrated at 110 °C for 1 h under an Ar flow and was quickly heated to 200 °C and kept at this temperature for 1 h. Under the Ar blanket, the solution was heated to reflux for 1 h before it was cooled down to room temperature. The Fe_3O_4 NPs were separated and purified as described.[15]

Coating NPs with Phospholipid. A portion of the as-synthesized NPs (2−5 mg) in 1 mL of chloroform was mixed and shaken with 10 mg of DSPE-PEG(2000)carboxylic acid lipid (1 mL of chloroform solution) (MW = 2847.779, Avanti Polar Lipids Inc.) for 10 min. The solvent was removed through rotavaporation. DI water or PBS buffer was then added to disperse the NPs. The NPs were further purified by a 100k dialysis tubing (Spectrum Laboratories, Inc.), and the final product, FePt−COOH or Fe_3O_4−COOH, was filtered through a 0.22 μm Millex@GP filter (Millipore Corp.) to remove small amounts of aggregates. The final NP concentration was determined with ICP-AES.

Fe (or Pt) Release Experiment. A portion (2 mL) of the aqueous solution of the phospholipid-coated NPs (FePt−COOH or Fe_3O_4−COOH) containing 1 mg of Fe were dispersed in dialysis tubing (MWCO = 1000, Spectrum Laboratories, Inc.) that was further immersed into a 30 mL PBS (pH = 7.4 or 4.8) bath at 37 °C. A portion (1 mL) of the PBS solution was sampled, and the concentration of Fe or Pt was analyzed with ICP-AES.

Characterization of ROS Formation. A2780 cells were placed at a density of 20 000 cells per well into black 96-well plates and were incubated at 37 °C in 5% CO_2 and high humidity for 24 h. Cells were loaded with DCFH-DA (10 μM in HBSS, 0.5% DMSO (v/v)) and were incubated at 37 °C in 5% CO_2 and high humidity for 30 min. The probe was removed, and the cells were washed twice with PBS (200 μL). The cells were then kept in Hanks' Balanced Salt Solution (HBSS), and the phospholipid-coated NPs (FePt−COOH or Fe_3O_4−COOH) were diluted with HBSS and added to the wells. The fluorescence spectrum was recorded every 15 min over a period of 6 h at 37 °C via excitation at 480 nm and emission at 538 nm on a BMG FLUO star plate reader.

Fluorescent Microscopic Examination of ROS with DCFH-DA as Indicator. For the fluorescent microscopic examination, A2780 cells were plated onto coverslips (Corning) in 12-well plates. Cells monolayer grown on glass coverslips were allowed to near confluence and then placed on ice; the medium was aspirated, and the cells were washed twice with PBS. Then, cells were prestained with 20 μM DCFH-DA in PBS for 30 min and washed with PBS to remove the free DCFH-DA. Later, the cells were incubated with NPs or other reagents for 2 h before they were washed with PBS for three times and fixed with 4% formaldehyde in PBS for 10 min. The coverslips with cells on the surface were removed from the wells and mounted onto slides using 90% glycerol in H_2O. The images were acquired by a Leica TCS SP2 AOBS spectral confocal microscope with excitation at 488 nm and emission from 510−550 nm.

Characterization of Lipid Oxidation. A2780 cells were stained with a 10 μM solution of C11-BODIPY in HBSS (prepared from the stock solution 10 mM C11-BODIPY in methanol) for 30 min prior to NP treatment in HBSS buffer. The probe was removed, and the cells were washed twice with PBS. The cells were kept in HBSS, and the NPs were diluted with HBSS (Fe: 1.5 ppm; Pt: 7.6 ppm) and added to the wells. The fluorescence spectrum was recorded every 30 min over a period of 6 h at 37 °C (nonoxidized: λ_{ex} = 581 nm, λ_{em} = 595 nm; oxidized: λ_{ex} = 485 nm, λ_{em} = 520 nm).

(12) (a) Halliwell, B.; Gutteridge, J. M. C. *Biochem. J.* **1984**, *219*, 1–14. (b) Valko, M.; Rhodes, C. J.; Moncol, J.; Izakovic, M.; Mazur, M. *Chem. Biol. Interact.* **2006**, *160*, 1–40. (c) Papanikolaou, G.; Pantopoulos, K. *Toxicol. Appl. Pharmacol.* **2005**, *202*, 199–211. (d) Graf, E.; Mahoney, J. R.; Bryant, R. G.; Eaton, J. W. *J. Biol. Chem.* **1984**, *259*, 3620–3624. (e) Braughler, J. M.; Duncan, L. A.; Chase, R. L. *J. Biol. Chem.* **1986**, *261*, 282–289. (f) Imlay, J. A.; Linn, S. *Science* **1988**, *240*, 1302–130.

(13) Dharap, S. S.; Wang, Y.; Chandna, P.; Khandare, J. J.; Qiu, B.; Gunaseelan, S.; Sinko, P. J.; Stein, S.; Farmanfarmaian, A.; Minko, T. *Proc. Natl. Acad. Sci. U.S.A.* **2005**, *102*, 12962–12967.

(14) Chen, M.; Liu, J. P.; Sun, S. H. *J. Am. Chem. Soc.* **2004**, *126*, 8394–8395.

(15) Sun, S. H.; Zeng, H. *J. Am. Chem. Soc.* **2002**, *124*, 8204–8205.

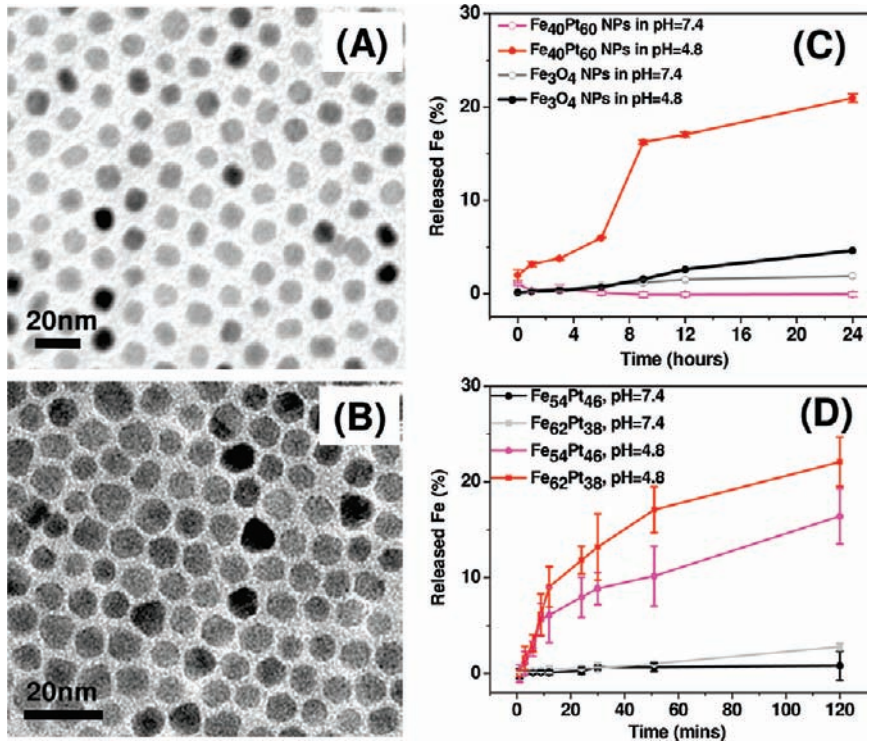

Figure 1. TEM images of the as-synthesized (A) 9 nm fcc-$Fe_{40}Pt_{60}$ NPs and (B) 9 nm Fe_3O_4 NPs, respectively. (C) Fe release from the fcc-$Fe_{40}Pt_{60}$ and Fe_3O_4 NPs in PBS at different pHs. (D) Fe release from FePt NPs with different compositions in PBS at both low (4.8) and high (7.4) pHs.

Fluorescent Microscopic Examination of Lipid Peroxidation with C11-BODIPY. For the fluorescent microscopic examination, similar steps were used as in the ROS measurement except that DCFH-DA was replaced with C11-BODIPY.

Cytotoxicity Assay (MTT Assay). Colorimetric MTT (3-(4,5-dimethylthiazol-2-yl)-2,5-diphenyl tetrazolium bromide, Sigma) assays were performed to assess the mitochondrial activity of cells treated as the following. The cytotoxicity assay was performed in 96-wells microtiter plates (Fisher Inc.) with a seeding density of 4000 cells per well. Microtiter plates containing cells were preincubated for 24 h at 37 °C in order to allow stabilization before the addition of the test substance. The plates were incubated with the test substance for 24 h at 37 °C in 5% CO_2. Then, 100 μg/mL MTT solution (DMEM) was added to each well to evaluate cell viability after the NPs solution was removed. After 2 h at 37 °C, MTT solution was removed. DMSO (100 μL) was added to dissolve the cells. After a 30 min incubation at 37 °C, the plate was measured using 550 nm as the test wavelength and 630 nm as the reference wavelength on a microreader (SpectraMax 340PC384, Molecular Devices). Viability was calculated based on the recorded data.

TEM Sample Preparation. After being incubated with NPs for 4 h and washed with PBS, the cells were detached with 0.05% trypsin EDTA and fixed with modified Karnovsky's Fixative (2% paraformaldehyde and 2% gluteraldehyde in PBS) before they were postfixed in 1% OsO_4 for 1.5 h, stained with 2% uranyl acetate for 2 h, and dehydrated in alcohol and propylene oxide. The treated cells were then embedded in Eponate resin, sectioned with an ultramicrotome, and mounted on the 150 mesh TEM grids. The sections were stained again with uranyl acetate (25 min) and lead citrate (10 min) for TEM image analysis. The images were acquired from a Philips EM 420 at 80 kV.

Coupling LHRH or $CH_3-PEG_4-NH_2$ to FePt NPs. EDC (0.4 mg, 2 mM) and sulfo-NHS (1.1 mg, 5 mM) were incubated with FePt−COOH NPs (10 mg) in water for 15 min. 2-Mercaptoethanol (1.4 μL) was added to inactivate excessive EDC. The sulfo-NHS−NP intermediate was separated with a PBS pre-equilibrated PD-10 column (GE Healthcare). LHRH peptide (0.5 mg) or $CH_3-PEG-NH_2$ (0.08 mg) was added to the sulfo-NHS−NPs and reacted for 2 h at room temperature. The final product, abbreviated as FePt−LHRH or FePt−CH_3, was purified with a PD-10 column. The coupling of LHRH was characterized by matrix-assisted laser desorption/ionization (MALDI) mass spectrometry (Applied Biosystem, Voyager-DE PRO, BioSpectrometry Workstation).

Results and Discussion

Fe-catalyzed H_2O_2 decomposition is known as Fenton's reaction in which highly reactive oxygen species (ROS), such as the hydroxyl radical (•OH), are generated. These ROS are a powerful agent for oxidizing various organic molecules including membrane lipids, DNA, and proteins in cells. Therefore, a mismanagement of Fe in cellular systems can lead to the toxic Fe buildup and the resultant production of ROS, causing oxidative stress, cellular damage, and cell death.[12] To better control this Fe buildup process for cancer therapy, we proposed to use FePt NPs as an Fe reservoir to release toxic Fe in specifically targeted tumor cells. As a test, we prepared 9 nm fcc-FePt NPs by previously reported procedures with modification.[14] The composition of Fe and Pt was controlled by the ratio of $Fe(CO)_5$ and $Pt(acac)_2$ during the synthesis and was measured by ICP-AES. We also prepared 9 nm Fe_3O_4 NPs[15] and used them as a control. TEM images of the 9 nm fcc-$Fe_{40}Pt_{60}$ NPs and the 9 nm Fe_3O_4 NPs are given in Figure 1A, B. The as-synthesized NPs were coated with a layer of oleate and oleylamine and were made water-soluble through surfactant addition of the commercially available phospholipid.[16] The phospholipid forms a bilayer-locked structure through the hydrocarbon chains of oleate/oleylamine. This double layer

(16) (a) Medintz, I. L.; Uyeda, H. T.; Goldman, E. R.; Mattoussi, H. *Nat. Mater.* **2005**, *4*, 435–446. (b) Dubertret, B.; Skourides, P.; Norris, D. J.; Noireaux, V.; Brivanlou, A. H.; Libchaber, A. *Science* **2002**, *298*, 1759–1762. (c) Hultman, K. L.; Raffo, A. J.; Grzenda, A. L.; Harris, P. E.; Brown, T. R.; O'Brien, S. *ACS Nano* **2008**, *2*, 477–484.

efficiently stabilizes the NPs in aqueous solutions. The hydrodynamic size of these modified NPs was measured to be 60 nm in PBS and 80 nm in PBS + 10% fetal bovine serum (FBS) at pH 7.4 (Figure S1 of the Supporting Information). The NPs remained stable during the 72 h incubation (37 °C) period.

The pH-dependent Fe release from the phospholipid modified fcc-FePt NPs was analyzed in PBS with pH 7.4, the pH value of body fluid and cytoplasm, and pH 4.8, the pH value of the lysozome.[17] The fcc-FePt NPs were suspended in dialysis tubing and incubated at 37 °C in PBS with pH 4.8 and 7.4. The Fe_3O_4 NPs with the same modification were used as a control. Fe and Pt released from the NPs were measured by analyzing samples removed from the reservoir solution at different time intervals with ICP-AES. The etching results are shown in Figure 1C, D. At pH = 7.4, both 9 nm fcc-$Fe_{40}Pt_{60}$ NPs and 9 nm Fe_3O_4 NPs have no measurable Fe in the solution outside the dialysis tubing within 24 h. However, the fcc-FePt NPs at pH = 4.8 have a 17% Fe release after ~8 h, while the Fe_3O_4 NPs have only very small amount of Fe ion released within 24 h of incubation (Figure 1C). To characterize the release of the Fe from different FePt NPs, fcc-FePt NPs with different Fe and Pt compositions as described previously were prepared at ratios of $Fe_{62}Pt_{38}$ and $FePt_{54}Pt_{46}$ and tested in solutions at both pH 7.4 and pH 4.8. For the same FePt NPs, they have negligible Fe release at pH = 7.4, while at pH = 4.8, Fe-rich FePt NPs tend to release more Fe into solution (Figure 1D). In addition to Fe analysis, Pt concentrations were measured concurrently using ICP-AES. During the experimental analysis, free Pt ion was not detected from the FePt NPs under the same incubation conditions (Figure S2 of the Supporting Information). These results indicate that, unlike metallic Fe NPs that are easily oxidized,[18] the fcc-FePt NPs act as an Fe reservoir that protects Fe from oxidation/release under pH found in serum (pH 7.4). However, Fe is released under low pH conditions found in the cellular lysozome (pH 4.8). Results in Figure 1C demonstrate that the Fe release from the $Fe_{40}Pt_{60}$ NPs is slower relative to other FePt NPs tested in the low pH condition, allowing appreciable release of Fe in a longer time frame.

The released Fe from the fcc-$Fe_{40}Pt_{60}$ NPs initiated the catalytic formation of ROS in A2780 cells. The ROS concentration increase in A2780 was characterized by 2′,7′-dichlorodihydrofluorescein diacetate (DCFH-DA) reaction,[19] as shown in Figure 2A. Briefly, DCFH-DA is incubated with the cells in the media. Following cellular uptake, two ester groups in DCFH-DA are hydrolyzed to hydroxyl groups in the presence of intracellular esterase. In the presence of ROS, DCFH is deprotonated and converted to quinone-like DCF that fluoresces at 480 nm excitation. The A2780 cells were incubated with DCFH-DA in the presence of fcc-FePt NPs or the control Fe_3O_4 NPs at an Fe concentration of 1.5 μg/mL in Hank's Buffered Salt Solution (HBBS). The fcc-FePt NPs exhibited a 50% higher intensity after 6 h in culture compared to cells incubated with the Fe_3O_4 NPs (Figure 2B). This enhanced fluorescence was further visualized through the bright green fluorescent image of the cells (Figure 2C), indicating the formation of DCF. In contrast, the green fluorescent images from the cells incubated with Fe_3O_4 NPs and DCFH-DA were much weaker (Figure S3 of the Supporting Information) and close to that from the A2780 cells not incubated with the NPs. These experiments prove that the fcc-FePt NPs induce the formation of excess ROS in A2780 cells.

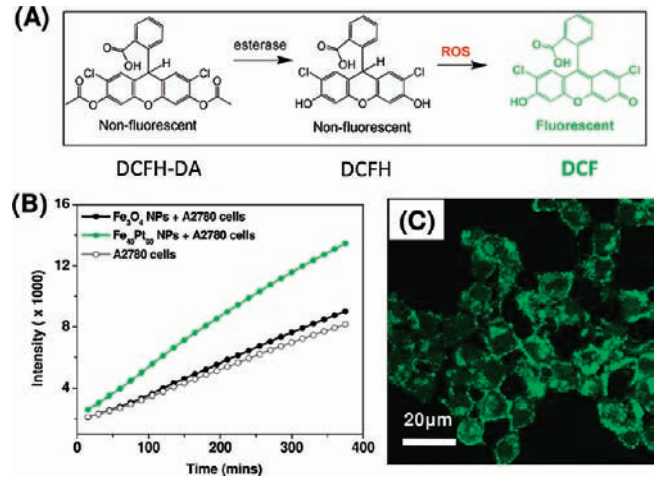

Figure 2. (A) Schematic illustration of DCFH-DA conversion to DCF. (B) Time-dependent fluorescent intensity from DCFH-DA labeled A2780 cells with fcc-FePt and Fe_3O_4 NPs (Fe concentration: 1.5 μg/mL) in HBSS. (C) Green fluorescent image of DCFH-DA labeled A2780 cells after incubation with fcc-$Fe_{40}Pt_{60}$ NPs for 2 h.

The excessive production of ROS within cells can lead to rapid lipid oxidation, DNA and protein damage, and eventually cell death.[12] Here, we assessed the membrane lipid damage via the oxidation of a fluorescent dye 4,4-difluoro-5-(4-phenyl-1,3-butadienyl)-4-bora-3*a*,4*a*-diaza-*s*-indacene-3-undecanoic acid (C11-BODIPY, Molecular Probes) (Figure 3A).[20] C11-BODIPY inserts into the cell membrane, and the oxidation of the carbon−carbon double bonds by ROS decreases the emission of C11-BODIPY at 595 nm. In the experiment, the C11-BODIPY labeled A2789 cells treated with fcc-$Fe_{40}Pt_{60}$ NPs show weaker emission at 595 nm, correlating with C11-BODIPY oxidation (Figure 3B). The lipid membrane damage caused by fcc-$Fe_{40}Pt_{60}$ NPs was also evidenced through the fluorescent images of the A2780 cells incubated only with C11-BODIPY (Figure 3C), which were brighter, and those incubated with both C11-BODIPY and fcc-$Fe_{40}Pt_{60}$ NPs (Figure 3D), which were darker due to the C11-BODIPY oxidation. In comparison, the A2780 incubated with the control Fe_3O_4 NPs had emissions at 595 nm similar to those without Fe_3O_4 NP treatment, indicating less membrane oxidation (Figure 3B). A2780 cells visualized by TEM following incubation with the fcc-FePt NPs demonstrated a lack of internal membrane bound vesicles (Figure 3E), suggesting lipid membrane destruction following NP uptake. In contrast, A2780 cells incubated with the Fe_3O_4 NPs cells showed clearly the demarcated endosomal-lysozomal vesicles, indicating no lipid membrane oxidation (Figure S4 of the Supporting Information).

The FePt-initiated catalytic formation of ROS results in serious toxicity to various cells. MTT viability testing was used to assess the toxicity of the FePt NPs. Viability testing was conducted in several representative cell lines including A2780, HeLa, A431 (human epithelial carcinoma cell line), Sk-Br3

(17) Demaurex, N. *News Physiol. Sci.* **2002**, *17*, 1–5.
(18) Peng, S.; Wang, C.; Xie, J.; Sun, S. H. *J. Am. Chem. Soc.* **2006**, *128*, 10676–10677.
(19) Lebel, C. P.; Ischiropoulos, H.; Bondy, S. C. *Chem. Res. Toxicol.* **1992**, *5*, 227–231.
(20) (a) Drummen, G. P. C.; van Liebergen, L. C. M.; Op den Kamp, J. A. F.; Post, J. A. *Free Radic. Biol. Med.* **2002**, *33*, 473–490. (b) Halliwell, B.; Whiteman, M. *Br. J. Pharmacol.* **2004**, *142*, 231–255.
(21) Kohanski, M. A.; Dwyer, D. J.; Hayete, B.; Lawrence, C. A.; Collins, J. J. *Cell* **2007**, *130*, 797–810.

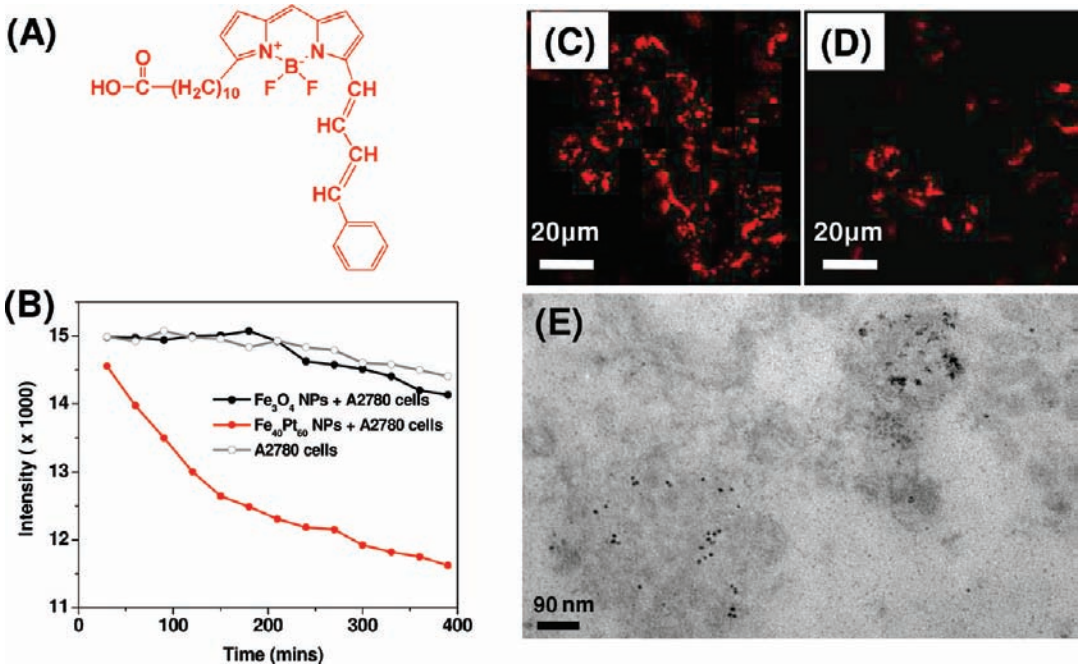

Figure 3. (A) Structure of C11-BODIPY. (B) Fluorescent emission intensity detected at 595 nm from C11-BODIPY labeled A2780 cells and those treated with $Fe_{40}Pt_{60}$ or Fe_3O_4 NPs. (C, D) Fluorescent images of the A2780 cells after treatment with C11-BODIPY alone (C) and those treated with C11-BODIPY and incubation with $Fe_{40}Pt_{60}$ NPs (D) for 2 h. (E) TEM image of a cross section of an A2780 cell after treated with $Fe_{40}Pt_{60}$ NPs for 4 hrs.

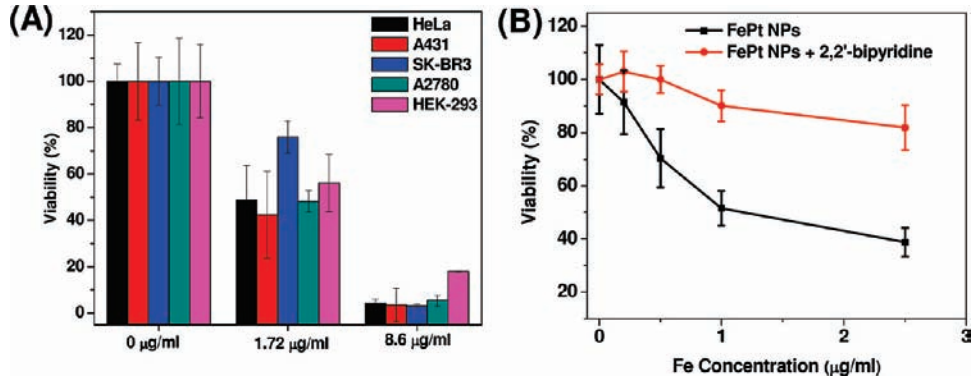

Figure 4. (A) MTT cellular viability of several tumor cell lines incubated with fcc-$Fe_{40}Pt_{60}$ NPs at different iron concentrations at 37 °C for 24 h. (B) Viability of A2780 cells incubated with fcc-$Fe_{40}Pt_{60}$ NPs or with fcc-$Fe_{40}Pt_{60}$ NPs plus 200 μM 2,2′-bipyridine at 37 °C for 24 h.

(human breast cancer cell line), and HEK-293 (human embryonic kidney cell line). As shown in Figure 4A, incubation of these cells with the fcc-$Fe_{40}Pt_{60}$ NPs produced a dose-dependent reduction in cell viability at Fe concentrations of 1.72 μg/mL and 8.6 μg/mL. For A2780 cells, the fcc-$Fe_{40}Pt_{60}$ NPs have an IC_{50} of 1.25 μg Fe/mL (Figure 4B).

In principle, the production of ROS, and therefore the toxicity of the NPs, can be blocked with an intracellular iron chelator. In this experiment, we chose 2,2′-bipyridine, an iron chelator that has been used to capture Fe within bacteria to reduce the formation of ROS,[21] to assess whether the cells could be "rescued" from ROS generated by the FePt NPs. Initially, 2,2′-bipyridine was tested in A2780 cells and shown to be nontoxic at concentrations up to 500 μM (Figure S5 of the Supporting Information). Cells incubated with the FePt NPs and 200 μM 2,2′-bipyridine demonstrated a 50% higher viability in culture than cells cultured without the 2,2′-bipyridine (Figure 4B). These results indicate that ROS generated by the release of Fe from the FePt NPs can be chelated by the 2,2′-bipyridine, reducing the production of ROS through catalytic decomposition of H_2O_2.

To maximum therapeutic efficacy induced by the fcc-FePt NPs, these NPs must be able to target a specific tumor site. Luteinizing hormone-releasing hormone (LHRH) peptide was chosen as a model targeting agent to test targeting capabilities of the fcc-$Fe_{40}Pt_{60}$ NPs. It is known that LHRH receptors (LHRHRs) are overexpressed on breast, ovarian, and prostate cancer cells and are not detectable on most visceral organs.[22] In the experiments, we first coupled LHRH peptide to fcc-$Fe_{40}Pt_{60}$ NPs via the common EDC/sulfo-NHS chemistry. The coupling was confirmed by MALDI mass spectrometry (Figure S6 of the Supporting Information). Using similar chemistry, we also deactivated the fcc-$Fe_{40}Pt_{60}$–COOH with $CH_3-PEG_4-NH_2$, in which the methyl group has little binding ability onto the cell surface.[22] Thus, the fcc-

(22) (a) Emons, G.; Schally, A. V. *Hum. Reprod.* **1994**, *9*, 1364–1379. (b) Bentzen, E. L.; Tomlinson, I. D.; Mason, J.; Gresch, P.; Warnement, M. R.; Wright, D.; Sanders-Bush, E.; Blakely, R.; Rosenthal, S. J. *Bioconjugate Chem.* **2005**, *16*, 1488–1494.

(23) (a) Gao, J. H.; Liang, G. L.; Cheung, J. S.; Pan, Y.; Kuang, Y.; Zhao, F.; Zhang, B.; Zhang, X. X.; Wu, E. X.; Xu, B. *J. Am. Chem. Soc.* **2008**, *130*, 11828–11833. (b) Maenosono, S.; Suzuki, T.; Saita, S. *J. Magn. Magn. Mater.* **2008**, *320*, L79–L83.

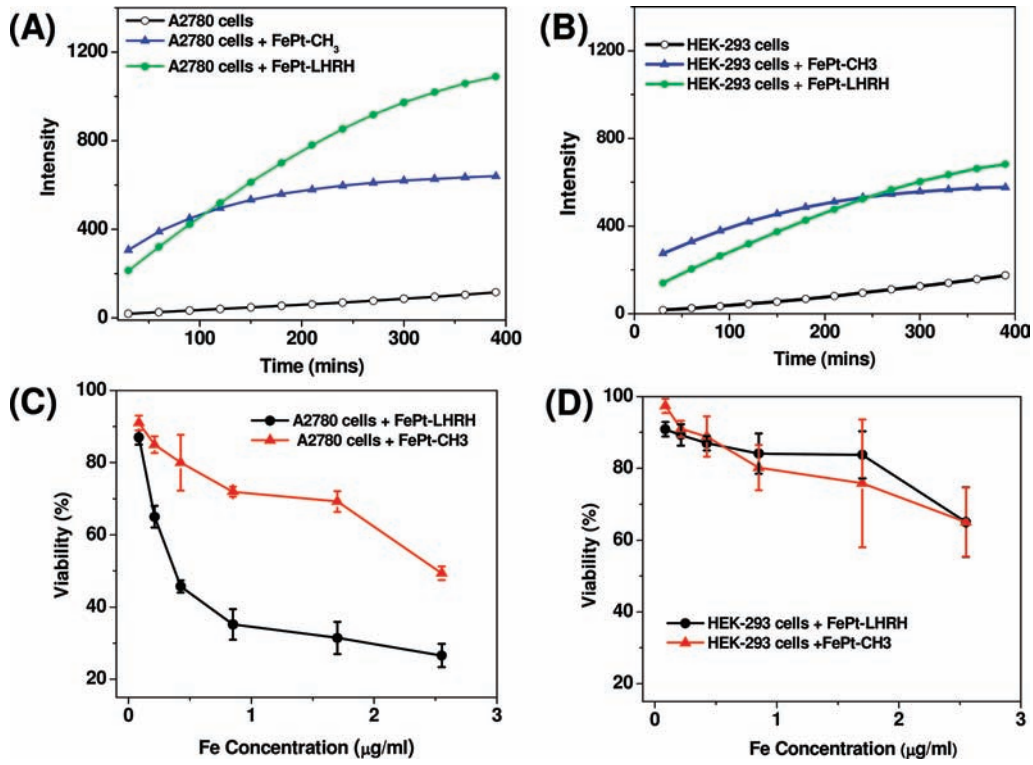

Figure 5. (A, B) Fluorescent intensity of DCF from A2780 (A) and HEK-293 cells (B). (C, D) MTT viability assay of A2780 (C) and HEK-293 (D) cells incubated with the FePt−LHRH or FePt−CH_3 NPs.

$Fe_{40}Pt_{60}$−COONH−PEG_4−CH_3 (FePt−CH_3) NPs could be used as a control. A2780 cells that overexpress LHRHRs and HEK-293 cells (human embryonic kidney) that have low LHRHR expression were chosen for cell targeting experiments.[13,22] To characterize ROS induced by the FePt NPs in the A2780 and HEK-293 cells, DCFH-DA dye was used as described in Figure 2. As predicted by previous experiments, the fluorescent intensity is increased in LHRH-targeted A2780 cells relative to the HEK-298 cells (Figure 5A, B). To assess the viability of the cells targeted with LHRH peptide, MTT viability analysis was conducted on A2780 and HEK-293 cells incubated with the FePt NPs. A2780 cells incubated with the targeted FePt NPs (FePt−LHRH) showed a lower viability compared to A2780 cells incubated with the FePt−CH_3 NPs (Figure 5C). In addition, HEK-293 cells incubated with both FePt−CH_3 and FePt−LHRH showed a higher viability (Figure 5D) than the A2780 cells incubated with the FePt−LHRH NPs presumably due to the low expression of LHRH receptors on the cell surface. The conjugation of LHRH to the FePt NPs reduced their IC_{50} from 2.5 μg/mL (FePt−CH_3) (Figure 5C) and 1.25 μg/mL (FePt−COOH) (Figure 4B) down to 0.4 μg/mL (FePt−LHRH) (Figure 5C) due to the overexpression of the LHRH receptor. The difference in the generation of ROS (Figure 5A, B) and cellular viability (Figure 5C, D) can be attributed to the preferential uptake of FePt−LHRH NPs through the LHRH receptor. Thus, cellular targeting can enhance the cytotoxicity of the FePt NPs due to a higher avidity for the cell surface and higher intracellular uptake.

Finally, as an additional control, A2780 cells were incubated with fcc-FePt NPs that were pre-etched in PBS buffer at pH = 4.8 for 24 h to deplete Fe. A2780 cells incubated with these pre-etched NPs showed a higher viability compared to cells incubated with those FePt NPs preincubated in neutral buffer for 24 h (Figure S7 of the Supporting Information). This further indicates that (1) ROS, and the related cellular cytotoxicity, are generated through the elution of Fe from the FePt NPs and (2) Pt-rich (postetched) FePt NPs should not have appreciable cytotoxicity to cellular systems before their elimination from biological systems following the destruction of their tumor cell target. Therefore, with the targeted delivery of catalytic Fe, the fcc-FePt NPs should serve as a promising therapeutic agent.

Conclusion

In this work, we have presented an exciting new therapeutic property of the phospholipid coated fcc-FePt NPs, their controlled release of Fe for catalytic H_2O_2 decomposition and production of ROS, which is toxic to tumor cells. Once conjugated with the LHRH peptide, the FePt NPs show the enhanced cytotoxicity in cells overexpressing the LHRH receptors. The more important aspects are that fcc-FePt NPs, as a new type of therapeutic agent, can in principle be coated and conjugated with various kinds of lipid molecules, peptides, and antibodies that are specific for other tumor cell types. Therefore, through rational surface functionalization, the fcc-FePt NPs can be well-conditioned with high therapeutic efficacy to any tumor cells that can be targeted. This, plus their contrast enhancement capability in magnetic resonance imaging (MRI),[23] should warrant fcc-FePt NPs a powerful agent for future imaging guided cancer therapy.

Acknowledgment. The work was supported by NIH/NCI 1R21CA12859.

Supporting Information Available: Nanoparticle characterization and interactions with cells. This material is available free of charge via the Internet at http://pubs.acs.org.

JA905938A